Edge state reconstruction from strong correlations in quantum spin Hall insulators

Edge states reconstruction from strong correlations in quantum spin Hall insulators

A. Amaricci, L. Privitera, F. Petocchi, and M. Capone
Scuola Internazionale Superiore di Studi Avanzati (SISSA) and Democritos National Simulation Center, Consiglio Nazionale delle Ricerche, Istituto Officina dei Materiali (IOM), Via Bonomea 265, 34136 Trieste, Italy

G. Sangiovanni and B. Trauzettel
Institut für Theoretische Physik und Astrophysik, Universität Würzburg, Am Hubland, D-97074 Würzburg, Germany

(Dated: February 22, 2017)

We study quantum spin Hall insulators with local Coulomb interactions in the presence of boundaries using dynamical mean field theory. We investigate the different influence of the Coulomb interaction on the bulk and the edge states. Interestingly, we discover an edge reconstruction driven by electronic correlations. The reason is that the helical edge states experience Mott localization for an interaction strength smaller than the bulk one. We argue that the significance of this edge reconstruction can be understood by topological properties of the system characterized by a local Chern marker.

Introduction.– Topological insulators are symmetry-protected quantum materials with a gapped bulk but gapless edge states. In two spatial dimensions, the quantum spin Hall insulator (QSHI) is the prime example of a topologically non-trivial phase of matter. Here, the underlying symmetry that needs to be preserved is time-reversal symmetry (TRS) [1–3]. The QSHI phase is usually detected by transport properties determined by its boundary modes, which are coined helical edge states [4–6] because their spin degree of freedom and their direction of motion are strongly coupled to each other. This leads to a protection from elastic backscattering off potential fluctuations [7, 8]. However, in experiments, edge state transport in the QSHI is not perfect implying some sort of backscattering mechanism. The interplay of Coulomb interaction and spin-mixing disorder has been proposed as a possible origin of such inelastic backscattering [9–14]. Thus, it is crucial to better understand the influence of Coulomb interaction on the physical properties of QSHIs. In fact, already for bulk systems, i.e. in the absence of edge states, it has been shown that topological insulators in the presence of strong Coulomb interaction behave rather differently as compared to their weakly or non-interacting counterparts [15–25].

In this article we address the problem of how the helical edge states in a strongly interacting QSHI phase are affected by Coulomb interaction. Using dynamical mean-field theory (DMFT) [26, 27], we study the role of Coulomb interaction in a paradigmatic model of the QSHI, called Bernevig-Hughes-Zhang (BHZ) model [3], in a stripe geometry. We show that the influence of electronic correlation is more pronounced at the boundaries than in the bulk. This perception is nicely illustrated by the evolution of the quasiparticle weight Z, which coincides with the inverse of the effective mass enhancement within DMFT, as a function of the interaction strength U for the first few layers ($y = 1$ being the outermost one), see Fig. 1. For non-topological systems, it has been

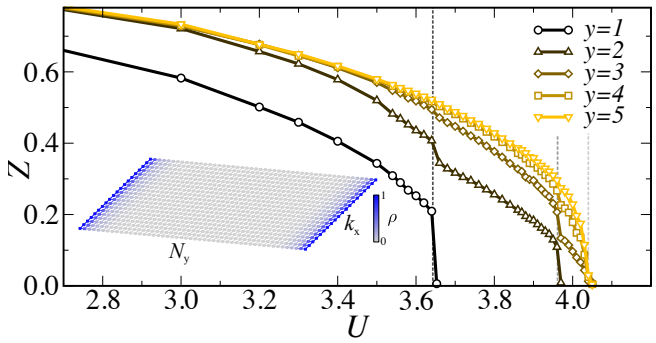

Figure 1. Quasiparticle weight Z as a function of the interaction strength U for the first few layers (under the parameter choice $M = 1$ and $\lambda = 0.3$ of the BHZ model, see Eq. (1) below). The vertical dashed lines indicate the Mott localization of the first three layers, signaled by $Z_y = 0$. Inset: schematic representation of the stripe system. Points of the lattice are colored according to the corresponding value of the spectral weight $\rho = A_y(k_x, \omega = 0)$.

realized before that Mott localization can happen more efficiently at the boundary of a given system than in the bulk because the kinetic energy is effectively reduced at the edge [28]. However, for the QSHI this result has a new implication. Since the Mott localization of the outer helical edge state happens for a smaller interaction strength than that of the bulk, the bulk itself remains in the QSHI phase. Hence, the Mott insulator at the boundary acts as a new vacuum (still preserving TRS) resulting in a new topological edge state that is moved inside the QSHI system. To the best of our knowledge, this is the first example of a topological edge reconstruction triggered by Coulomb interaction.

Model and Method.– We consider a two-orbital BHZ model supplemented by a local interaction term [19, 23]. The model is defined on a two-dimensional stripe system formed by a finite number N_y of one-dimensional layers stacked along the y direction with open boundary

conditions (OBC). We assume translational invariance and periodic boundary conditions (PBC) along the x direction (see inset of Fig.1). We introduce the following Γ-matrices: $\Gamma_0 = \mathbb{1}\otimes\mathbb{1}$, $\Gamma_x = \sigma_z\otimes\tau_x$, $\Gamma_y = -\mathbb{1}\otimes\tau_y$, $\Gamma_5 = \mathbb{1}\otimes\tau_z$, $\Gamma_\sigma = \sigma_z\otimes\mathbb{1}$, where $\sigma_{x,y,z}$ and $\tau_{x,y,z}$ are two sets of Pauli matrices acting, respectively, on the spin and orbital sector, $\otimes$ is the usual tensor product, and $\mathbb{1}$ is the 2×2 identity matrix. Then, the model Hamiltonian reads

$$H = \sum_{k_x,y,y'} \Psi^\dagger_{k_x y}\mathbf{M}(k_x)\delta_{yy'}\Psi_{k_x y'} + \sum_{k_x y,y'}\left(\Psi^\dagger_{k_x y}\mathbf{T}\delta_{y+1y'}\Psi_{k_x y'} + H.c.\right) + H_{\rm int}\ , \quad (1)$$

where k_x is the first component of the wave-vector, $y = 1,\dots,N_y$ is the coordinate in the y direction (i.e. the layer index), $\mathbf{M}(k_x) = (M-\epsilon\cos(k_x))\Gamma_5 + \lambda\sin(k_x)\Gamma_x$, $\mathbf{T} = -\frac{\epsilon}{2}\Gamma_5 + i\frac{\lambda}{2}\Gamma_y$ and $\Psi^\dagger_{k_x y} = (c^\dagger_{1\uparrow}, c^\dagger_{2\uparrow}, c^\dagger_{1\downarrow}, c^\dagger_{2\downarrow})_{k_x y}$ where the first index refers to the orbital degree of freedom. The first two terms in Eq. (1) describe a system of two bands of width $W = 6\epsilon$, hybridized with an amplitude λ and separated in energy by a splitting of $2M$. In the following, we consider a total density of two electrons per site, i.e. a system at half-filling. We assume ϵ as our energy unit and choose $\lambda = 0.3$ and $M = 1$ (if not stated differently).

The last term of the model Hamiltonian describes a local Coulomb interaction with both *inter-* and *intra-*orbital repulsion and the Hund's coupling J, taking into account the exchange effect which favors high-spin configurations. In terms of the local operators, $\hat{N} = \sum_{\mathbf{ij}}\Psi^\dagger_{\mathbf{i}}\Gamma_0\delta_{\mathbf{ij}}\Psi_{\mathbf{j}}$, $\hat{S}_z = \frac{1}{2}\sum_{\mathbf{i}}\Psi^\dagger_{\mathbf{i}}\Gamma_\sigma\delta_{\mathbf{ij}}\Psi_{\mathbf{j}}$, $\hat{T}_z = \frac{1}{2}\sum_{\mathbf{i}}\Psi^\dagger_{\mathbf{i}}\Gamma_5\delta_{\mathbf{ij}}\Psi_{\mathbf{j}}$, the interaction term reads:

$$H_{\rm int} = (U-J)\frac{\hat{N}(\hat{N}-1)}{2} - J\left(\frac{\hat{N}^2}{4} + \hat{S}_z^2 - 2\hat{T}_z^2\right)\ , \quad (2)$$

where U is the strength of the electron-electron interaction and $\Psi_{\mathbf{i}=x,y} = \sqrt{\frac{2\pi}{V}}\sum_{k_x} e^{-ik_x\cdot x}\Psi_{k_x y}$. [29]. In the remainder of the article, we fix $J = U/4$ but none of our results are specific to this choice.

We solve the interacting problem non-perturbatively using DMFT, focusing on non-magnetic solutions. This choice implies that Coulomb interaction will not lift the TRS protecting the QSHI phase. Anti-ferromagnetic ordering, which can be expected at low temperature in the absence of frustration, would instead break TRS leading to a different boundary scenario beyond the scope of the present work. In order to capture the different behavior between bulk and boundaries, we use an extension of DMFT to treat inhomogeneous systems [30–32]. In this framework, the interaction effect is contained in layer-dependent self-energy functions $\Sigma_y(\omega)$, bearing the correct spin-orbital structure. From this quantity we compute the layer-dependent quasiparticle weight $Z_y = (1-\partial{\rm Re}\Sigma_y(\omega)/\partial\omega_{|_{\omega\to0}})^{-1}$, which coincides in DMFT with the inverse of the effective mass enhancement and it is a direct measure of the localization effect induced by the interactions. In non-interacting systems, $Z_y = 1$, while $0 < Z_y < 1$ denotes systems with finite electronic correlations; $Z_y = 0$ is the hallmark of Mott localization.

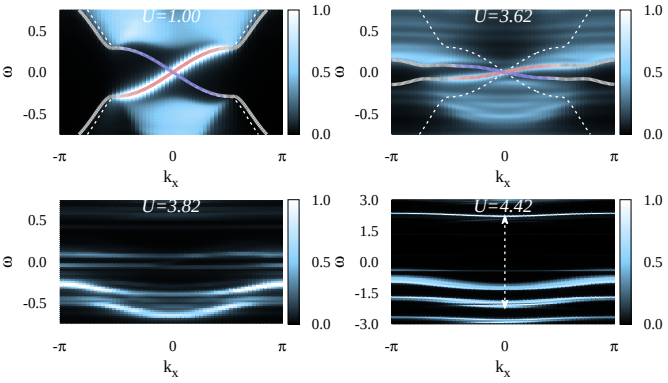

Figure 2. Evolution of the low-energy spectral function $A_y(k_x,\omega)$ (of the first orbital and spin up) for different interaction strength U. The dashed and solid (red and blue) lines indicate, respectively, the bare and the renormalized dispersion relation of the helical edge states. In the last panel the arrow indicates the width of the Mott gap.

Results.– In the non-interacting regime, $U = J = 0$, the BHZ model (in its lattice-regularized version) describes a topological quantum phase transition (TQPT) for $M = 2$, separating a trivial Band Insulator (characterized by a topological invariant $\nu = 0$) for $M > 2$ from a QSHI (with topological invariant $\nu = 1$) for $M < 2$ [19]. In the QSHI phase the model hosts helical edge states localized at the two boundaries of the stripe, as shown in the inset of Fig.1, where we report the zero-frequency local spectral weight for the non-interacting system, which is finite for the edge states and vanishes in the bulk. In the bulk, the combined effect of the interaction terms U and J is to favor the equal population of the two bands, effectively reducing the energy splitting M [19, 23]. This favors the QSHI over the trivial insulator, but it also changes the character of the transition in the strongly interacting regime from continuous to first-order [23–25]. Finally, a large enough interaction strength drives the transition to a topologically trivial high-spin Mott state [23, 24]

In this work, we consider the stripe geometry introduced above. In this geometry, the correlation effects acquire a spatial modulation because of the existence of boundaries, breaking the translational symmetry in the y direction. This can be understood noticing that the electrons at the boundary layers can not hop in the outside direction. They have therefore a reduced kinetic energy with respect to electrons in the bulk, which makes the

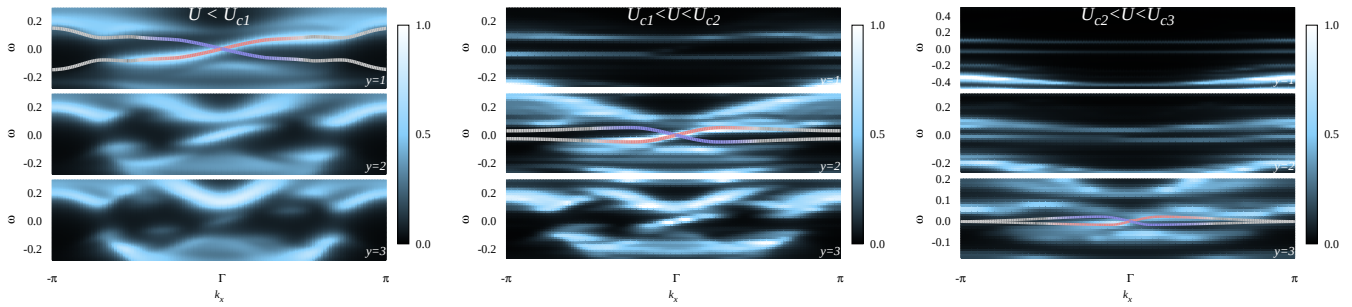

Figure 3. Evolution of the spectral functions $A_y(k_x,\omega)$ (of the first orbital and spin up) for the first three layers $y=1,2,3$ (in the corresponding rows) as a function of the interaction strength $U=3.62<U_{c1}$ (left), $U_{c1}<U=3.82<U_{c2}$ (center) and $U_{c2}<U=3.98<U_{c3}$ (right). For clarity of presentation, we picked just one orbital and one spin degree of freedom. The limited spatial extent of the edge states of about three layers can be nicely seen. The solid lines (red and blue) indicate the renormalized helical edge states dispersion (depicted for all spin-orbital channels to emphasize their helical character).

interaction terms more effective at the edges. This effect is shown in Fig.1, reporting the layer-resolved quasiparticle weight Z_y as a function of the interaction strength U. In the weak-coupling regime ($U=1$), the effect of the Coulomb interaction is to just renormalize the bands, without affecting the qualitative nature of the QSHI solution. Upon increasing the interaction strength, we observe the progressive reduction of the Z_y's. The boundary value Z_1 is the smallest and Z_y increases approaching the bulk layers. Most interestingly, Z_1 abruptly vanishes at $U_{c1}\simeq 3.64$, significantly smaller than the bulk Mott transition point. Further increasing the interaction strength, Z_2 vanishes abruptly at a second critical interaction $U_{c2}>U_{c1}$, eventually followed by the other layers. The successive critical points U_{cy}, where Z_y vanishes, appear to rapidly accumulate to a U_c^{stripe} still smaller than the bulk critical interaction strength (that we have previously determined [19, 23]). At the critical interaction strengths U_{cy}, all the inner layers show a little jump in their quasiparticle weights. We can thus conclude that the value U_c^{stripe}, where all the quasiparticle weights vanish, is the critical interaction strength for a full Mott localization of the whole QSHI stripe.

In order to get insight on the critical points U_{cy} we study the evolution of the low-energy part of the spectral function, which contains the single-particle excitations of the correlated system. To avoid excessively busy figures, we plot only the contribution from one orbital and one spin degree of freedom to $A_y(k_x,\omega)\equiv -\frac{1}{\pi}\mathrm{Im}G_{y\,m=1\,\uparrow}(k_x,\omega+i0^+)$, because the other components contain exactly the same physical information and can be reconstructed by symmetry.

In Fig.2, we report the evolution of the boundary spectral function $A_1(k_x,\omega)$. The figure shows that the helical edge states are renormalized by Z_1 for $U<U_{c1}$ and they discontinuously disappear at U_{c1}, leaving behind a small low-energy gap which turns into a large Mott-like gap of order U only for values of the interaction strength $U>U_c^{stripe}$, see the last panel in Fig.2. Therefore, the jump of Z_1 at U_{c1} can be described as a selective localization transition in which the delocalized helical edge states undergo some form of Mott localization, preceding the full Mott transition of the bulk. Analogously, U_{c2} marks a similar selective Mott localization for the second layer, and so on.

In the intermediate regime, comprised between the gap opening of the edge states and the Mott transition, the system opposes to the strong interaction with a *contraction* of the bulk and a *reconstruction* of the helical edge states. This is the central result of our work. To demonstrate this effect, we report in Fig.3 the evolution of the spectral function $A_y(k_x,\omega)$ and the renormalized gapless edge states for the first few layers across the multiple transition points indicated in Fig.1. For small values of the interaction strength ($U=3.62<U_{c1}$, left column), the system is characterized by the presence of helical edge states localized at the outermost layer and a gapped bulk. Increasing the interaction strength above the first critical point ($U_{c1}<U=3.82<U_{c2}$, middle column), this opens a gap in that first layer. This process is accompanied by the formation of a new pair of helical edge states in the neighboring internal layer as to preserve the topologically non-trivial character of the system against Coulomb interaction, according to the bulk-boundary correspondence. Further increasing the interaction strength ($U_{c2}<U=3.98<U_{c3}$, right column) causes a gap opening also in the second layer with the collapse of the gapless helical states which again are reconstructed in the adjacent layer. The bulk contraction and edge state reconstruction process end when the interaction strength becomes too large to prevent the reformation of renormalized helical edge states. At this point, a large Mott gap penetrates the system, transforming it into a trivial Mott insulator. We next substantiate our explanation of the edge reconstruction by a topology analysis.

Topological Invariant.– The topological nature of the QSHI is described by the global invariant $\nu\in\mathbb{Z}_2$ [1, 33].

In presence of TRS and conserved spin $\nu = (\mathcal{C}_\uparrow - \mathcal{C}_\downarrow)/2 \bmod 2$, where $\mathcal{C}_\sigma$ is the Chern number for a given spin channel σ. The value of $\mathcal{C}_\sigma$ is usually expressed as a suitable integral over the Brillouin zone [20, 34]. However, the topological character can also be obtained in real space (Wannier) representation using a different, yet equivalent, formulation originally introduced by Bianco and Resta [35, 36], which is particularly useful in presence of OBC. The key idea is to rewrite the Chern number in real space as [37]

$$\mathcal{C}_\sigma = \lim_{V\to\infty} \frac{1}{V} \int_V d\mathbf{r}\; 2\pi i \langle \mathbf{r}| \left(\hat{x}^\sigma_{\mathcal{P}} \hat{y}^\sigma_{\mathcal{Q}} - \hat{y}^\sigma_{\mathcal{P}} \hat{x}^\sigma_{\mathcal{Q}} \right) |\mathbf{r}\rangle \qquad (3)$$

where $\hat{x}^\sigma_{\mathcal{P}} = \mathcal{P}^\sigma \hat{x} \mathcal{Q}^\sigma$ and $\hat{y}^\sigma_{\mathcal{Q}} = \mathcal{Q}^\sigma \hat{y} \mathcal{P}^\sigma$ are the projected position operators, and $\mathcal{P}^\sigma$ and $\mathcal{Q}^\sigma$ are, respectively, the projectors onto the occupied and empty bands of spin σ of the topological Hamiltonian [34]. The integrand of Eq. (3) defines the local Chern marker (LCM) $C_\sigma(x, y)$ [35, 36]. For a finite system the right hand side of Eq. (3) exactly vanishes. However, the *nearsighted* nature [38, 39] of the electronic wave functions guarantees that the LCM coincides with the Chern number in the bulk of a sufficiently large system. Deviations from this value can appear at the boundary of the non-trivial sample to insure the vanishing of the integral (3) [40]. Thus, all the information about the topological nature of our stripe system is provided by the LCM $C_\sigma(x, y)$ [35, 37, 41].

A crucial prerequisite of the observed edge reconstruction (driven by Coulomb interaction) is the preservation of the non-trivial topological character in the interior part of the stripe. The reconstructed helical edge states then separate the QSHI in the spatially shrunken bulk from the Mott gapped external layers. In order to illustrate this point, we evaluate the LCM $C_\sigma(x, y)$, with x the coordinate conjugated to k_x in a finite lattice of dimension $N_x \times N_y$. The bulk averages of $C_\sigma(x, y)$ give the $\mathbb{Z}_2$ topological invariant characterizing the QSHI state. The evolution of the LCM distribution across the Mott transition is reported in Fig.4. In the non-trivial phase, the $C_\sigma(x, y)$ undergo positive and negative oscillations at the boundary which cancel out the bulk contribution to the integral (3), see top panel in Fig.4. However, such oscillations are not present in the trivial phase (see bottom panel). This enables us to discriminate between trivial and non-trivial parts of the same system. Indeed in the intermediate regime preceding the full Mott localization, the LCM of the external layers becomes zero whereas the non-trivial part with $\nu = 1$ is compressed towards the bulk.

Conclusions. – We have studied the properties of the edge states in a BHZ model in the presence of strong (on-site) Coulomb interactions. Our analysis shows that the correlation-driven transition from a QSHI to a Mott insulator occurs through a series of selective localization transitions as the interaction grows, before the bulk eventually turns into a Mott insulating state. At each localization transition the outermost helical edge states are gapped by the interaction. The disappearance of the helical modes at the outer layer is accompanied by a reconstruction of new (renormalized) edge states at the immediately inner layers. This phenomenon demonstrates the survival of a topologically non-trivial QSHI state in the bulk – a direct consequence of the bulk-boundary correspondence. Our results show that novel physics can be seen in theoretical approaches able to treat simultaneously bulk and boundaries of correlated topological materials.

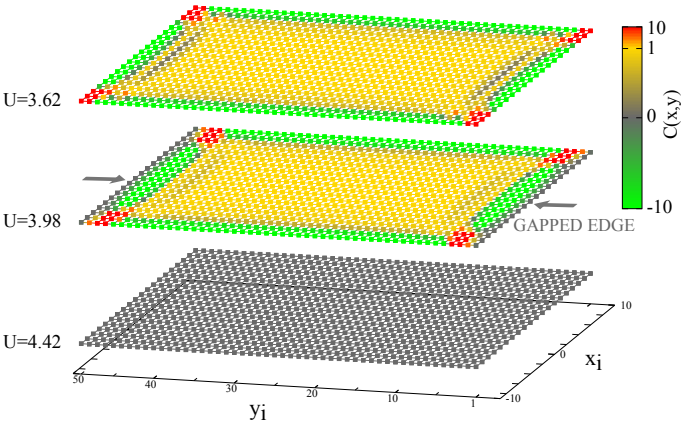

Figure 4. Spatial distribution of the Chern marker $C_{\sigma=\uparrow}(x, y)$ for different values of the interaction strength U. Data is shown for a finite lattice with dimensions $N_x \times N_y = 20 \times 50$ with PBC along x and OBC along y. Each point of the system is colored according to the value of $C_\uparrow$. Top layer: The marker has constant value $C_\uparrow = 1$ in the bulk. Oscillations at the border are a feature of the Chern marker in the non-trivial phase, but do not appear in the trivial one. Middle layer: The marker is $C_\uparrow = 1$ in the bulk, but gapped edge states at $y = 1, 50$ have $C_\uparrow = 0$. Bottom layer: The marker is identically zero in the trivial Mott state.

Acknowledgments. – We thank J.C. Budich for interesting discussions and a critical reading of the manuscript. A.A., F.P., and M.C. acknowledge financial support from MIUR through the PRIN 2015 program (Prot. 2015C5SEJJ001), the Seventh Framework Programme FP7, under Grant No. 280555 "GO FAST", and the H2020 Framework Programme, under ERC Advanced Grant No. 692670 "FIRSTORM". G.S. and B.T. acknowledge financial support by the DFG (SPP 1666 on "Topological Insulators" and SFB 1170 "ToCoTronics").

[1] C. L. Kane and E. J. Mele, Phys. Rev. Lett. **95**, 146802 (2005).
[2] C. L. Kane and E. J. Mele, Phys. Rev. Lett. **95**, 226801 (2005).
[3] B. A. Bernevig, T. L. Hughes, and S.-C. Zhang, Science **314**, 1757 (2006).

[4] M. Knig, S. Wiedmann, C. Brne, and *et al.*, Science **318**, 766 (2007).
[5] A. Roth, C. Brüne, H. Buhmann, L. W. Molenkamp, J. Maciejko, X.-L. Qi, and S.-C. Zhang, Science **325**, 294 (2009).
[6] I. Knez, R.-R. Du, and G. Sullivan, Phys. Rev. Lett. **107**, 136603 (2011).
[7] C. Wu, B. A. Bernevig, and S.-C. Zhang, Phys. Rev. Lett. **96**, 106401 (2006).
[8] C. Xu and J. E. Moore, Phys. Rev. B **73**, 045322 (2006).
[9] A. Ström, H. Johannesson, and G. I. Japaridze, Phys. Rev. Lett. **104**, 256804 (2010).
[10] J. C. Budich, F. Dolcini, P. Recher, and B. Trauzettel, Phys. Rev. Lett. **108**, 086602 (2012).
[11] F. Crépin, J. C. Budich, F. Dolcini, P. Recher, and B. Trauzettel, Phys. Rev. B **86**, 121106 (2012).
[12] T. L. Schmidt, S. Rachel, F. von Oppen, and L. I. Glazman, Phys. Rev. Lett. **108**, 156402 (2012).
[13] J. I. Väyrynen, M. Goldstein, and L. I. Glazman, Phys. Rev. Lett. **110**, 216402 (2013).
[14] F. Geissler, F. Crépin, and B. Trauzettel, Phys. Rev. B **89**, 235136 (2014).
[15] S. Rachel and K. Le Hur, Phys. Rev. B **82**, 075106 (2010).
[16] M. Hohenadler, T. C. Lang, and F. F. Assaad, Phys. Rev. Lett. **106**, 100403 (2011).
[17] M. Hohenadler and F. F. Assaad, Phys. Rev. B **85**, 081106 (2012).
[18] Y. Tada, R. Peters, M. Oshikawa, A. Koga, N. Kawakami, and S. Fujimoto, Phys. Rev. B **85**, 165138 (2012).
[19] J. C. Budich, B. Trauzettel, and G. Sangiovanni, Phys. Rev. B **87**, 235104 (2013).
[20] M. Hohenadler and F. F. Assaad, Journal of Physics: Condensed Matter **25**, 143201 (2013).
[21] H.-H. Hung, V. Chua, L. Wang, and G. A. Fiete, Phys. Rev. B **89**, 235104 (2014).
[22] F. Lu, J. Zhao, H. Weng, Z. Fang, and X. Dai, Phys. Rev. Lett. **110**, 096401 (2013).
[23] A. Amaricci, J. C. Budich, M. Capone, B. Trauzettel, and G. Sangiovanni, Phys. Rev. Lett. **114**, 185701 (2015).
[24] A. Amaricci, J. C. Budich, M. Capone, B. Trauzettel, and G. Sangiovanni, Phys. Rev. B **93**, 235112 (2016).
[25] B. Roy, P. Goswami, and J. D. Sau, Phys. Rev. B **94**, 041101 (2016).
[26] A. Georges, G. Kotliar, W. Krauth, and M. J. Rozenberg, Rev. Mod. Phys. **68**, 13 (1996).
[27] G. Kotliar, S. Y. Savrasov, K. Haule, and *et al.*, Rev. Mod. Phys. **78**, 865 (2006).
[28] G. Borghi, M. Fabrizio, and E. Tosatti, Phys. Rev. Lett. **102**, 066806 (2009).
[29] This Hamiltonian only contains the "density-density" part of the Hund's exchange and neglects the so-called pair-hopping and spin-flip terms. The robustness of the topological transitions in the BHZ model against the pair-hopping and spin-flip terms has been verified in Ref. 19.
[30] M. Potthoff and W. Nolting, Phys. Rev. B **60**, 7834 (1999).
[31] J. K. Freericks, *Transport in Multilayered Nanostructures* (Imperial College Press, London, 2006).
[32] A. Amaricci, A. Privitera, and M. Capone, Phys. Rev. A **89**, 053604 (2014).
[33] C. L. Kane and M. J. E., Physics World **24**, 32 (2011).
[34] Z. Wang and S.-C. Zhang, Phys. Rev. X **2**, 031008 (2012).
[35] R. Bianco and R. Resta, Phys. Rev. B **84**, 241106 (2011).
[36] R. Bianco, *Chern invariant and orbital magnetization as local quantities*, Ph.D. thesis, Università degli studi di Trieste (2014).
[37] L. Privitera and G. E. Santoro, Phys. Rev. B **93**, 241406 (2016).
[38] W. Kohn, Phys. Rev. Lett. **76**, 3168 (1996).
[39] R. Resta, The European Physical Journal B **79**, 121 (2011).
[40] The integral (3) can vanish either trivially, because the integrand is identically zero as for the Mott insulator, or in a non-trivial way as for the QSHI.
[41] D.-T. Tran, A. Dauphin, N. Goldman, and P. Gaspard, Physical Review B **91**, 085125 (2015).